

# THERMAL BLOOMING OF POWERFUL LASERS IN PURE WATER AND CLEAREST SALTWATERS

**A.A. Aboul Enein**  
**F.Z. El-Halafawy**  
Fac. of Elect. Eng.,  
Menoufia, Univ.,  
Menouf, 32952, Egypt.

**E.A. El-Badawy**  
Fac. of Eng. King Saud Univ.,  
Riyadh, Saudi Arabia.

**N.M. Wassef**  
Fac. Eng., Alex., Univ.,  
Alexandria, Egypt.

## ABSTRACT

The interaction of a powerful laser beam and an unguided channel (pure water and clearest saltwater) has been rigorously investigated through the average beamwidth parameter. A special numerical technique is designed taking into account the coupling of the beam and the medium along the propagation path. The physical parameters of the medium are considered as temperature-dependent and frequency-dependent parameters. The beam divergence has been deeply analyzed in order to reduce it through the affecting set of parameters (beam power, radius, and frequency).

## I. INTRODUCTION

The interactions of both light and laser on the surface and within the sea, have recently been attracted in the last decade, through both military and civil applications such as the destruction of suspended and floated mines and the ice layers floating over the sea surface [1].

Marine optics concerned with the physical behaviour of such interactions [1,2] especially in the domain of classical optics where  $0.2 < \lambda < 1.0$  microns.

Optical energies undergo transmutations of a variety of types, such as:

- i- absorption, and therefore thermalization
- ii- scattering by particulates in suspension, and
- iii- photosynthesis and re-emission

In the optics of the sea, there are five substances that contribute to the optical properties; namely

- a- pure seawater,
- b- chlorophyll,
- c- yellow substances,
- d- detritus, and
- e- suspended materials.

The knowledge of the optical constants of seawater in the range of classical optics is of special importance to the heat balance of the earth as well as the remote sensing of the earth's atmospheric and surface features from satellites and to infrared signal transmission through the atmosphere near the surface of the sea [2,3].

The problem of powerful laser interaction with water is an extremely difficult one, because of a number of

different nonlinear phenomena such as shock waves, heating and evaporation [4,5]. The self-induced thermal distortion of the laser beam propagating in absorbing media is of special interest. The distortion of the laser beam is the result of heating of the path by absorption of a small fraction of the laser beam power by the medium which changes the refractive index and therefore distorts the beam leading to either self-focusing or defocusing of the beam [6]. There are many different types of thermal blooming, but generally the steady state blooming can be characterized by the form of heat transfer which is balancing the absorbed laser power. This phenomenon affects the required penetration depth (path). Thus, in the present paper, the thermal blooming of powerful lasers in either pure or salt waters is deeply analyzed and investigated on the basis of the average beam width parameter.

A trial is made to lengthen the penetration depth (path) through the irradiance tailoring, where the optical properties are considered both thermal and frequency-dependent. Also the coupling of the laser beam and the medium is considered all the way along the propagation path.

## *II- Optical Properties of Water.*

Optical oceanography has traditionally used the optical parameterization of the clearest possible ocean

waters as the baseline for the description and modelling of all oceanic light fields [7]. Jerlov [3] has classified the optical properties of various waters according to a scheme that divides them into oceanic (Type I to III) and coastal (Type 1 to 9) origins, based on their irradiance transmissivity in the upper 10 m. see Figure (1-a).

The clearest ocean water, type I, has been assumed in the present model.

### II.1. The thermal conductivity

Values of the scalar thermal molecular diffusivity [1] in the sea are of order  $1.49 \times 10^{-7} \text{ m}^2/\text{sec}$  while for pure water these values are of order  $1.569 \times 10^{-7} \text{ m}^2/\text{sec}$  [8]. Riley and Skirrow [9] reported the following equation for thermal conductivity (K) of sea water at salinity 34.994 % as a function of temperature and pressure under the form:

$$K = 0.55286 + 3.4025 \times 10^{-5} P + 1.8364 \times 10^{-3} (T - T_0) - 3.3058 \times 10^{-5} (T - T_0)^2 \text{ Watt m}^{-1} \text{ }^\circ\text{K}^{-1} \quad (1)$$

where P is the pressure in bars, T is the absolute temperature in  $^\circ\text{K}$ , and  $T_0$  is equal to  $273 \text{ }^\circ\text{K}$ .

Based on the data published in Reference [7], the following correlation is made for (K) of saturated liquid water

$$K = 0.54887 + 3.4025 \times 10^{-5} P + 2.67 \times 10^{-3} (T - T_0) - 1.4182 \times 10^{-5} (T - T_0)^2, \text{ Watt m}^{-1} \text{ }^\circ\text{K}^{-1} \quad (2)$$

### II.2. The heat transfer coefficient

The heat transfer coefficient of water as well as of seawater, h, is considered [8]

$$h = 1160 \text{ Watt m}^{-2} \text{ }^\circ\text{K}^{-1} \quad (3)$$

### II.3 The refractive index

Based on the data reported in References [9&10] the temperature dependence of the refractive index of pure water and seawater are cast under the form:

$$n(\lambda, T) = a_0 + a_1 (T - T_0) + a_2 (T - T_0)^2, \quad (4)$$

where  $a_0$  is a function of the optical wavelength while both  $a_1$  and  $a_2$  are constants. For pure water the computed values of  $a_1$  and  $a_2$  are

$$a_1 = 1.0804 \times 10^{-5} \text{ }^\circ\text{K}^{-1},$$

and

$$a_2 = -0.27010 \times 10^{-5} \text{ }^\circ\text{K}^{-2},$$

while for seawater:

$$a_1 = -4.5301 \times 10^{-5} \text{ }^\circ\text{K}^{-1},$$

and

$$a_2 = -0.14215 \times 10^{-5} \text{ }^\circ\text{K}^{-2}.$$

Algorithms for computing the fundamental properties of seawater, based on the practical salinity scale and the equation of state for seawater are reported by Fofonoff and Millard [11]

For simplicity and without lose of generality, the data reported by Austin and Halikas [12], Table I, are correlated to express the refractive index of pure water and of seawater as functions of wavelength and temperature under the form:

i- For pure water :

$$n_p = n_{op} + n_{1p} T + n_{2p} T^2 \quad (5)$$

with

$$n_{op} = 1.388468 - 1.5185 \times 10^{-4} \lambda + 1.003 \times 10^{-7} \lambda^2,$$

$$n_{1p} = -1.5825 \times 10^{-5} + 1.1222 \times 10^{-8} \lambda - 1.5872 \times 10^{-11} \lambda^2$$

and

$$n_{2p} = -2.0867 \times 10^{-6} + 3.1132 \times 10^{-10} \lambda - 1.11 \times 10^{-13} \lambda^2$$

ii- For seawater

$$n_s = n_{os} + n_{1s} T + n_{2s} T^2 \quad (6)$$

with

$$n_{os} = 1.397124 - 1.5691 \times 10^{-4} \lambda + 1.0383 \times 10^{-7} \lambda^2,$$

$$n_{1s} = -1.2838 \times 10^{-5} - 1.1611 \times 10^{-7} \lambda + 1.0217 \times 10^{-10} \lambda^2,$$

Table I. Selected data of the index of refraction, as a function of wavelength,  $\lambda$ , salinity and temperature at atmospheric pressure, used in constructing the index tables. Additional value at  $\lambda = 700$  nm and  $s = 34.998$  % have been estimated.

| $\lambda$<br>(nm) | S<br>(%) | CLOR<br>(%) | Temperature C |         |         |         |         |         |         |
|-------------------|----------|-------------|---------------|---------|---------|---------|---------|---------|---------|
|                   |          |             | 1.0           | 5.0     | 10.0    | 15.0    | 20.0    | 25.0    | 30.0    |
| 404.7             | 0.0      | 0.0         | 1.34375       | 1.34368 | 1.34348 | 1.34316 | 1.34274 | 1.34224 | 1.34166 |
|                   | 34.99    | 19.37       | 1.35093       | 1.35072 | 1.35040 | 1.34999 | 1.34950 | 1.34894 | 1.34831 |
| 435.8             | 0.0      | 0.0         | 1.34121       | 1.34114 | 1.34094 | 1.34062 | 1.34021 | 1.33971 | 1.33913 |
|                   | 34.99    | 19.37       | 1.34831       | 1.34811 | 1.34778 | 1.34736 | 1.34688 | 1.34632 | 1.34569 |
| 467.8             | 0.0      | 0.0         | 1.33913       | 1.33906 | 1.33886 | 1.33854 | 1.33813 | 1.33764 | 1.33706 |
|                   | 34.99    | 19.37       | 1.34615       | 1.34596 | 1.34563 | 1.34520 | 1.34471 | 1.34416 | 1.34355 |
| 480.0             | 0.0      | 0.0         | 1.33844       | 1.33837 | 1.33817 | 1.33786 | 1.33745 | 1.33695 | 1.33638 |
|                   | 34.99    | 19.37       | 1.34544       | 1.34525 | 1.34492 | 1.34450 | 1.34401 | 1.34345 | 1.34284 |
| 508.5             | 0.0      | 0.0         | 1.33701       | 1.33694 | 1.33674 | 1.33644 | 1.33603 | 1.33554 | 1.33497 |
|                   | 34.99    | 19.37       | 1.34397       | 1.34378 | 1.34344 | 1.34302 | 1.34253 | 1.34199 | 1.34138 |
| 546.1             | 0.0      | 0.0         | 1.33544       | 1.33537 | 1.33518 | 1.33487 | 1.33447 | 1.33398 | 1.33341 |
|                   | 34.99    | 19.37       | 1.34235       | 1.34215 | 1.34183 | 1.34140 | 1.34092 | 1.34037 | 1.33977 |
| 577.0             | 0.0      | 0.0         | 1.33434       | 1.33428 | 1.33408 | 1.33378 | 1.33338 | 1.33289 | 1.33233 |
|                   | 34.99    | 19.37       | 1.34122       | 1.34104 | 1.34070 | 1.34028 | 1.33979 | 1.33924 | 1.33865 |
| 579.1             | 0.0      | 0.0         | 1.33427       | 1.33421 | 1.33402 | 1.33371 | 1.33331 | 1.33282 | 1.33226 |
|                   | 34.99    | 19.37       | 1.34115       | 1.34097 | 1.34064 | 1.34021 | 1.33972 | 1.33917 | 1.33858 |
| 589.3             | 0.0      | 0.0         | 1.33395       | 1.33388 | 1.33369 | 1.33339 | 1.33299 | 1.33250 | 1.33194 |
|                   | 34.99    | 19.37       | 1.34081       | 1.34063 | 1.34030 | 1.33987 | 1.33938 | 1.33883 | 1.33824 |
| 643.8             | 0.0      | 0.0         | 1.33241       | 1.33234 | 1.33215 | 1.33186 | 1.33146 | 1.33098 | 1.33042 |
|                   | 34.99    | 19.37       | 1.33924       | 1.33905 | 1.33872 | 1.33830 | 1.33781 | 1.33726 | 1.33666 |
| 700.0             | 0.0      | 0.0         | 1.33109       | 1.33103 | 1.33084 | 1.33055 | 1.33016 | 1.32968 | 1.32913 |
|                   | 34.99    | 19.37       | 1.33788       | 1.33771 | 1.33738 | 1.33695 | 1.33644 | 1.33591 | 1.33532 |

$$n_{2s} = -2.4036 \times 10^{-6} + 3.1756 \times 10^{-9} \lambda - 2.5732 \times 10^{-12} \lambda^2$$

where  $1^\circ\text{C} < T - 273 < 30^\circ\text{C}$ , and  $400 < \lambda, \text{nm} < 700$ .

*II.4. The absorption coefficient*

The absorption coefficient of waters,  $a$ , (clearest natural waters or ocean water) had been recently reported as a frequency-dependent coefficient only [13-15] with a window of maximum penetration around  $\lambda = 450 \text{ nm}$ ; with a minimum absorption coefficient  $a_{\text{min}}$  equal to 0.0145 for clearest pure water. It had been noticed that for absorption, there is no significant difference between the fresh water and the clearest seawater. So the conclusion is that, sea salts exert little influence on light attenuation.

*III. Basic Model, Analysis, and Computational Technique*

The temperature  $T(r, z)$  is determined from the conduction dominated energy balance equation [6].

$$\nabla \cdot K_T \nabla T = -a I(r, z) \tag{7}$$

which is rewritten as

$$K \nabla^2 T + \partial k / \partial T [(\partial T / \partial r)^2 + (\partial T / \partial z)^2] = -a I(r, z) \tag{8}$$

The change in intensity  $I(r, z)$  of an initially collimated Gaussian laser beam propagating through inhomogeneous media whose refractive index  $n(r, z)$  has cylindrical symmetry around the propagation axis [15] is given as:

$$I(r, z) / I(r, 0) = \exp[-az - \int_0^z (\nabla_t + ((\nabla_t I) / I)) \times \int_0^z (\nabla_t n / n) dz' dz'] \tag{9}$$

Through a single characterizing parameter, namely the beamwidth parameter  $f(r, z)$ , the solution of Eqn. (9) is assumed under a simple closed form as:

$$I(r, z) = (I_0 / f^2) \exp[-(r^2 / R_0^2 f^2) - az] \tag{10}$$

where  $f(r, z)$  characterizes the diffraction pattern caused by the interaction of laser and the medium quantitatively and qualitatively where the following is found:

- i- At  $f < 1.0$ , the interaction causes focusing of the propagation path.
- ii- At  $f = 1.0$ , there is no interaction
- iii- At  $f > 1.0$ , the interaction causes defocusing along the propagation path.

Making the following substitution for dimensionless analysis (where  $R_0$  is the initial radius),

$$\rho = r / R_0, \eta = z / R_0, \partial / \partial r = d / R_0 \partial / \partial \rho$$

$$d / dz = d / R_0 \partial / \partial \eta, T_n = T(r, z) / T_0 = T_\rho e^{-a \rho^2}$$

$$K = K_0 [1 + \alpha (T_n - 1) + \beta (T_n - 1)^2]$$

in Eqn. (7) we obtain

$$K_n \nabla^2 T_n + K'_n [T_\rho'^2 + a^2 R_0^2 T_n^2] = - (I_n / R_0^2) e^{-a R_0 \eta} e^{-\rho^2 / f^2}$$

where

$$K_n = 1 + \alpha (T_n - 1) + \beta (T_n - 1)^2,$$

$$I_n = (a R_0^2 I_0) / (K_0 / T_0),$$

and,

$$K'_n = \alpha + 2 \beta (T_n - 1).$$

The boundary conditions required to solve Eqn. (10) are  $dT / d\rho = 0.0$  at  $\rho = 0.0$  and at the interface between the hot propagation path and the cold surrounding water i.e.,

$$\rho = \rho_w = R(\eta) / R_0, \text{ we have:}$$

$$-K \partial T_n / \partial \rho |_{\rho = \rho_w} = R_0 h (T_n - 1)$$

$\rho_w$  is called the marginal normalized radial position. Figure (1) The use of Eqn. (10) into Eqn. (9) yields



$$(f/\eta) (df/d\eta) = Af - B \quad (13)$$

where

$$A = (\nabla_t^2 n) / (2n)$$

and,

$$B = (\rho \nabla_t n) / n .$$

In this model Eqns.(11) and (13) are nonlinear coupled differential equations and are solved through step by step computational technique where Eqn. (13) is solved analytically at  $\eta$  and then Eqn. (11) is solved with the aid of finite difference at  $\eta + \nabla\eta$  with the initial condition  $f = 1$  at  $\eta = 0.0$ . The separation of variables and the integration of Eqn. (13) yield

$$f^2 = (B/A) + [1-(B/A)] e^{A\eta^2} \quad (14)$$

where A and B are temperature-dependent quantities through the thermal dependence of  $\nabla_t^2 n$ ,  $\nabla_t n$ , and n.

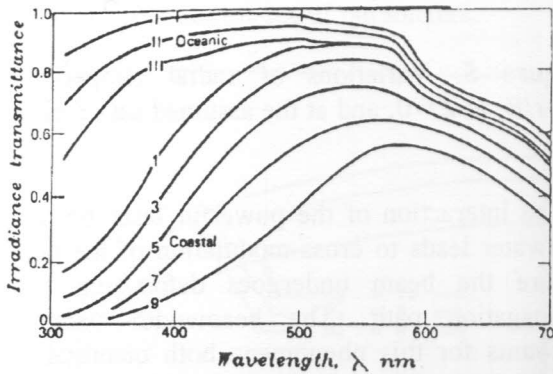


Figure 1-a. The spectral transmittance over the upper 10 m of water for jelov water types I to III 1 to 9 (adapted from jerlov, [3]).

$$\langle A \rangle = (1/\rho_\omega) \int_0^{\rho_\omega} ((\nabla_t^2 n)/2n) d\rho \quad (15)$$

$$\langle B \rangle = (1/\rho_\omega) \int_0^{\rho_\omega} ((\rho \nabla_t n) / n) df. \quad (16)$$

On the basis of Eqn.(14), the process of focusing or defocusing, in general, depends on the quantity (A-B). If this quantity is positive, the laser beam undergoes defocusing process, while the negativity of it leads to focusing process. The condition for stable beam propagation is: when:  $A = B$  which yields  $f(\eta) = 1.0$

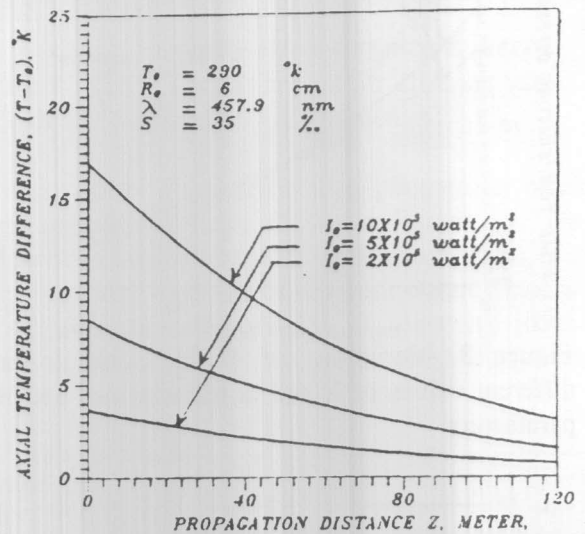


Figure 2. Variations of  $(T-T_0)$  with Z for different values of  $I_0$  and at the assumed set of parameters

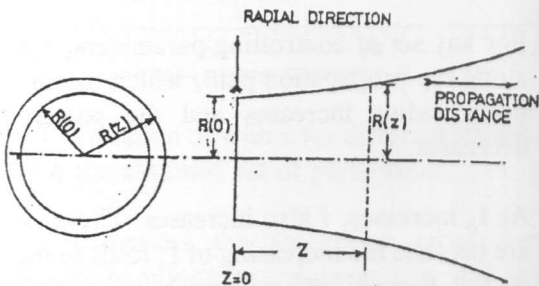


Figure 1-b. Geometrical model for laser propagation in static seawater.

The Processed computational technique handle the quantities A and B as average value over the beam cross-section i.e

#### IV: RESULTS AND DISCUSSION

A special algorithm is designed and employed to process the propagation phenomena of initially Gaussian powerful laser beam in either pure or salt-water, taking into account the thermal characteristics of the medium and the coupling of the laser beam and the medium along the propagation path. The variations of the axial temperature difference,  $(T-T_0)$ , against the propagation distance, Z, are displayed in Figures (2) and (3) for saltwater. These variations are of exponential nature due to the absorption loss given by Eqn. (11). As the optical wavelength  $\lambda$  increases, the attenuation increases, then  $(T-T_0)$  initially increases up to certain propagation

distance, and as the beam rapidly loses its power, the difference  $(T-T_0)$  decreases. As viewed from Eqn. (11), the increasing of  $I_0$  leads to increasing of the absorbed power, then at any propagation distance, the difference  $(T-T_0)$  increases. The radial temperature differences,  $(T-T_0)$  at the entrance of the laser beam of different powers are clarified in Figures (4) and (5) for saltwater. With the variations of either  $I_0$  or  $R_0$  or both,  $(T-T_0)$  have a monotonic variation along the radial position  $\rho$ .

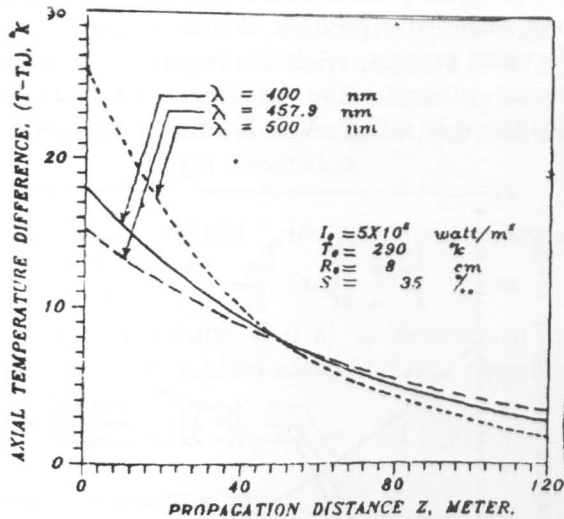


Figure 3. Variations of  $(T-T_0)$  with  $Z$  for different values of  $\lambda$  and at the assumed set of parameters.

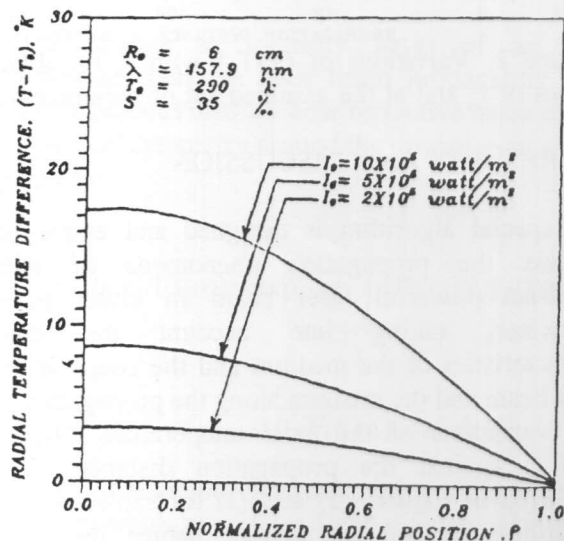


Figure 4. Variations of radial temperature with  $\rho=r/R$ , at  $Z=0$ , and at the assumed set of parameters.

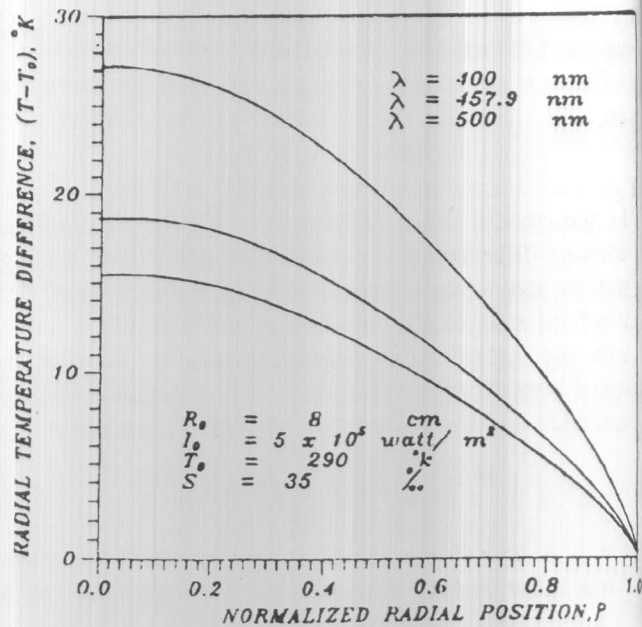


Figure 5. Variations of radial temperature with  $\rho=r/R$ , at  $Z=0$ , and at the assumed set of parameters.

The interaction of the powerful laser beam and the saltwater leads to cross-modulation of the laser beam where the beam undergoes defocusing along the propagation path. The beamwidth parameter,  $f$ , accounts for this phenomena both quantitatively and qualitatively. The variations of  $f$  against the variations of either  $I_0$  or  $R_0$  or  $\lambda$  along the propagation path are depicted in Figures (6) and (8). The main features of these variations are:

- i) For any set of controlling parameters,  $f$  increases along the propagation path, which means that the beam radius increases and the power density decreases.
- ii) As  $I_0$  increases,  $f$  also increases. These variations are because the increasing of  $I_0$  leads to increasing of the thermal effects which in turns leads to severe refractive index variations.
- iii) As  $R_0$  increases,  $f$  decreases whatever the propagation distance, although the power content in such case is relatively high

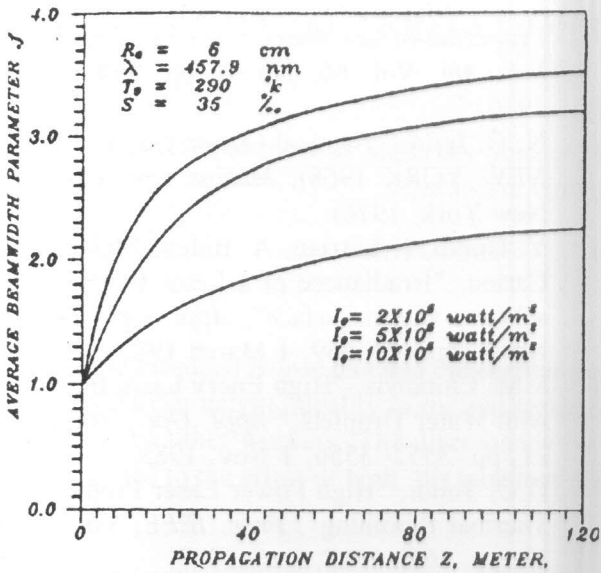


Figure 6. Variation of  $f$  with  $z$  for different values of  $I_0$ , and at the assumed set of parameters.

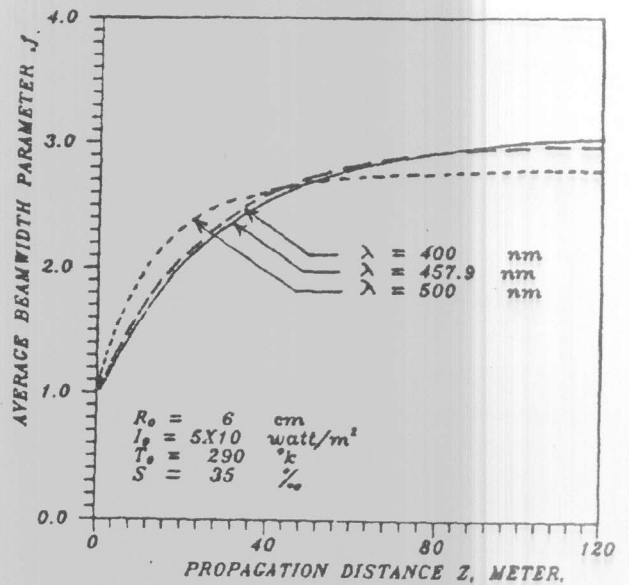


Figure 8. Variations of  $f$  with  $z$  for different values of  $\lambda$  and at the assumed set of parameters.

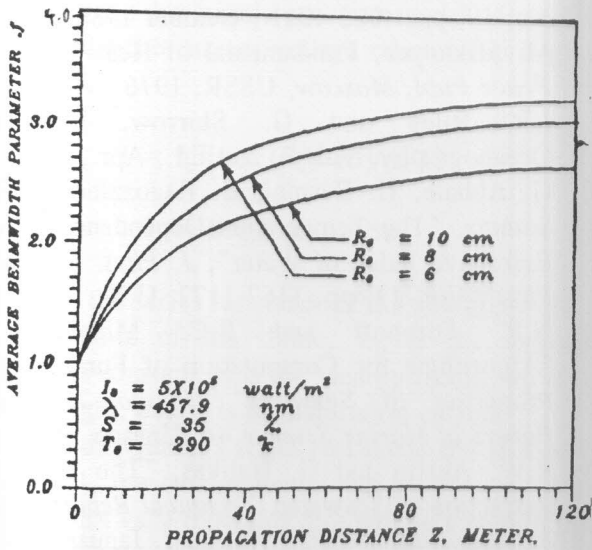


Figure 7. Variation of  $f$  with  $z$  for different values of  $R_0$ , and at the assumed set of parameters.

Comparisons of the defocusing phenomena in pure water and saltwater are shown in Figure (9). These comparisons indicate that the diffraction effect of sea water is greater than that of the pure water. Since with the salt, the thermal variation of refractive index is increasing by roughly 30 % over the fresh water values

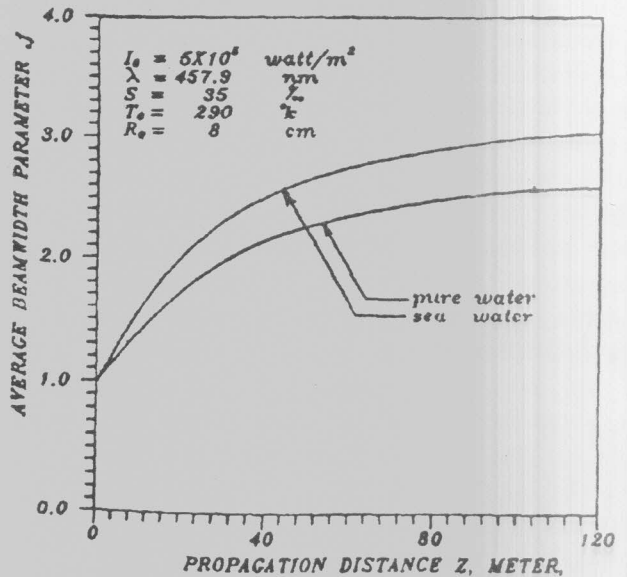
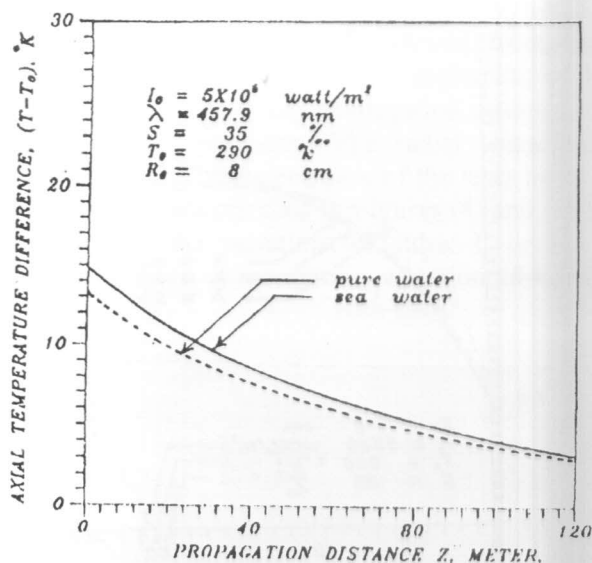


Figure 9. Variations of  $f$  with  $z$  for pure water and sea water at the assumed set of parameters.

- iv) As  $\lambda$  increases, the absorption cross section decreases to minimum values at  $\lambda = 457.9$  nm, then it increases again. The resulting thermal variations lead to the defocusing phenomena which is displayed in Figure (8)
- v) After a certain propagation distance,  $f$  tends to be constant, as the power density reaches to unaffected level, thus the thermal variations of the refractive index is of negligible weight.



**Figure 10.** Variation of  $(T-T_0)$  with  $Z$  for pure water and sea water at the assume set of parameters.

Finally, it is concluded that the beamwidth parameter acts as a simple but accurate dimensionless figure of merit to indicate the severity of the diffraction phenomena of powerful lasers in saltwaters.

## V. CONCLUSION

The interaction of powerful laser beams and water (pure or salt) are successfully processed through the dimensionless "beamwidth" parameter which accounts for the diffraction phenomena both qualitatively and quantitatively. A step-by-step technique is employed taking into consideration the thermal-dependence of the medium physical parameters and the coupling of the beam and the water along the propagation path. The "beamwidth" parameter is derived under a simple suitable closed form for the parametric investigation. The defocusing phenomena is studied over wide ranges of the affecting parameters. The conditions for maximum penetration keeping the level of power as high as possible, are clarified. The defocusing of powerful lasers in pure water is of less severity than in saltwater.

## REFERENCES

[1] J. R. Apel, "Principles of Ocean Physical, Ed. by W.L. Donn, AP, U.S.A, 1987.

- [2] L.W. Pinkly and D. Williams, "Optical Properties of Sea Water in the Infrared", *J. Opt. Soc. Am*, Vol. 66, No. 6, pp. 554-558, June 1976.
- [3] N. G. Jerlov, "Optical Oceanography (Elsevier, NEW YORK 1968); *Marine Optics* (Elsevier, New York, 1976).
- [4] Y. Guern, J. Lotrian, A. Bideau-Mehu, and J. Cariou, "Irradiance of a Laser Beam Through a Wavy Ocean surface", *Appl. Opt.*, Vol. 24, No. 5, pp. 655-659, 1 March 1985.
- [5] S.M. Chitanvis, "High Energy Laser Interactions with Water Droplets," *Appl. Opt.*, Vol.24, No. 21, pp. 3552- 3556, 1 Nov. 1985.
- [6] D.C. Smith, "High Power Laser Propagation : Thermal Blooming", *Proc. IEEE*, Vol.65, No. 12, pp. 1670-1715, Dec. 1977.
- [7] Robert H. Steven and Alan D. Weideman. "Optical Modelling of Clear Ocean light field: Raman Scattering effects" *Appl Opt.*, Vol. 27, No. 19, pp. 4002-4011 , October 1988.
- [8] M. Mikheyev, Fundamental of Heat Transfer, *Peace Publ, Moscow*, USSR, 1976.
- [9] J.P. Riley and G. Skirrow, Chemical Oceanography, Vol. 2, 2nd Ed., Apr., 1975.
- [10] G. Abbate, U. Bernini, E. Ragozzino and F. Somma, "The Temperature-Dependence of the Refractive Index of Water", *J. Phys. D: Appl. Phys.*, Vol. 11, pp. 1167-1172, U.K., 1978
- [11] N.P. Fofonoff and R.C. Millard Jr., "Algorithms for Computation of Fundamental Properties of Seawater" *Unesco Technical Papers in Marine Science 44*, Unesco 1983.
- [12] R.W. Austin and G. Halikas, "The Index of Refraction of Seawater, *Technical Report, Univ of California, SIO Ref. No. 76-1*, January 1976 U.S.A.
- [13] R.C. Smith, and K.S. Baker, "Optical Properties of the Clearest Natural Waters (200-800nm) " *Appl. Opt.* Vol. 20, No. 2, pp. 177-184, 15 Jan. 1981.
- [14] J.E. Tyler, "Optical Properties Of Water", Sec. 15 In: *Handbook of Optical Sponsored by OSA*, W.G.Drescooland W. Vaughan, Mc. Graw-Hill, U.S.A, 1978.
- [15] R.H.Staven, "Lambert-Bear Lawin Ocean Waters", *Appl.Opt.*, Vol.27 , No. 2, pp. 222-231, 15 Jan. 1988.